Biochimica et Biophysica Acta 1863 (2017) 857–869

Contents lists available at ScienceDirect

Biochimica et Biophysica Acta

journal homepage: www.elsevier.com/locate/bbadis

IL-6 promotes M2 macrophage polarization by modulating purinergic signaling and regulates the lethal release of nitric oxide during *Trypanosoma cruzi* infection

Liliana M. Sanmarco [a], Nicolás E. Ponce [a], Laura M. Visconti [b], Natalia Eberhardt [a], Martin G. Theumer [a], Ángel R. Minguez [b], Maria P. Aoki [a,*]

[a] Centro de Investigaciones en Bioquímica Clínica e Inmunología (CIBICI)-Consejo Nacional de Investigaciones Científicas y Tecnológicas (CONICET), Facultad de Ciencias Químicas, Universidad Nacional de Córdoba, Córdoba, Argentina
[b] Hospital Nuestra Señora de la Misericordia del Nuevo Siglo, Córdoba, Argentina

ARTICLE INFO

Article history:
Received 5 October 2016
Received in revised form 22 December 2016
Accepted 9 January 2017
Available online 11 January 2017

Keywords:
CD39
CD73
Human monocytes
Innate immunity

ABSTRACT

The production of nitric oxide (NO) is a key defense mechanism against intracellular pathogens but it must be tightly controlled in order to avoid excessive detrimental oxidative stress. In this study we described a novel mechanism through which interleukin (IL)-6 mediates the regulation of NO release induced in response to *Trypanosoma cruzi* infection. Using a murine model of Chagas disease, we found that, in contrast to C57BL/6 wild type (WT) mice, IL-6-deficient (IL6KO) mice exhibited a dramatic increase in plasma NO levels concomitant with a significantly higher amount of circulating IL-1β and inflammatory monocytes. Studies on mouse macrophages and human monocytes, revealed that IL-6 decreased LPS-induced NO production but this effect was abrogated in the presence of anti-IL-1β and in macrophages deficient in the NLRP3 inflammasome. In accordance, while infected WT myocardium exhibited an early shift from microbicidal/M1 to anti-inflammatory/M2 macrophage phenotype, IL6KO cardiac tissue never displayed a dominant M2 macrophage profile that correlated with decreased expression of ATP metabolic machinery and a lower cardiac parasite burden. The deleterious effects of high NO production-induced oxidative stress were evidenced by enhanced cardiac malondialdehyde levels, myocardial cell death and mortality. The survival rate was improved by the treatment of IL-6-deficient mice with a NO production-specific inhibitor. Our data revealed that IL-6 regulates the excessive release of NO through IL-1β inhibition and determines the establishment of an M2 macrophage profile within infected heart tissue.

1. Introduction

In response to different cardiac injuries, IL-6 is suddenly and continuously produced by cardiomyocytes and neighboring cells, suggesting that this cytokine is a fundamental part of the heart's intrinsic stress response system. It has been reported that the serum concentration of IL-6 increases after myocardial infarction [1] and in patients with congestive heart failure [2,3], as well as in hypertrophic and dilative cardiomyopathy [3]. Furthermore, systemic IL-6 levels correlate with the severity of left ventricular dysfunction and are strong independent predictors of subsequent clinical outcomes after myocardial infarction [1,2,4–7]. Previously, we have demonstrated that IL-6 drives the survival of cardiomyocytes infected by the cardiotropic protozoan parasite *Trypanosoma cruzi* [8,9]. Strikingly, our group and others have reported that mice deficient in IL-6 quickly succumb to *T. cruzi* infection [10,11]. These results suggest that an IL-6-dependent innate immune response is paramount for host survival. Although the biological importance of IL-6 in myocardial response is generally accepted, the mechanisms responsible for IL-6-dependent host protection in the infection setting have not yet been elucidated.

After injury the heart triggers leukocyte activation and recruitment. The first barrier of defense is constituted by cells of the myeloid lineage, which include neutrophils and monocytes/macrophages. Macrophage populations are particularly dynamic during inflammation or infection. Under such conditions, they can acquire two competing distinct functional phenotypes, which represent opposite extremes of a continuum ranging from classically activated M1 to alternatively activated M2 macrophages [12,13]. Classically activated M1 cells are efficient producers of pro-inflammatory cytokines (IL-1β, TNF, IL-6, IL-12) and NO which

* Corresponding author at: Haya de la Torre and Medina Allende, Ciudad Universitaria, CP 5000 Córdoba, Argentina.
E-mail addresses: lsanmarco@fcq.unc.edu.ar (L.M. Sanmarco), nponce@fcq.unc.edu.ar (N.E. Ponce), lau_visconti81@yahoo.com.ar (L.M. Visconti), neberhardt@fcq.unc.edu.ar (N. Eberhardt), mgtheumer@fcq.unc.edu.ar (M.G. Theumer), angelminguez04@yahoo.com.ar (Á.R. Minguez), paoki@fcq.unc.edu.ar (M.P. Aoki).

http://dx.doi.org/10.1016/j.bbadis.2017.01.006
0925-4439/

mediate antimicrobial effects and, in consequence, actively contribute to resistance against intracellular microorganisms. However, since inflammatory activity is potentially harmful, M1 macrophages need to be tightly controlled to avoid excessive tissue damage. To this aim, M2 macrophages dampen inflammation and promote tissue repair/remodeling and angiogenesis [14,15]. Indeed, M2 macrophages produce anti-inflammatory cytokines and trigger repair mechanisms, typically through arginase/ornithine/urea, EGF, VEGF, TGF-β and the mannose receptor (CD206). M1 and M2 macrophage signatures do not necessarily exclude each other and they often coexist *in vivo* [16]. In fact, *in vivo* macrophage cell function needs to be tailored to its tissue of residence, an adaptation that is driven by tissue-derived factors and by the physiological environment.

One important factor that can shape macrophage activation states in myocardium is the ATP metabolic machinery. Cardiac cells rapidly respond to hypoxic and inflammatory environment by releasing ATP (normally present within cardiomyocytes in millimolar concentration). Once released, ATP is converted to ADP/AMP and then to adenosine by the ectonucleoside triphosphate diphosphohydrolase-1 (CD39) and the ecto-5′-nucleotidase (CD73), respectively [17]. High levels of ATP act as a pro-inflammatory danger signal, activating the inflammasome that processes pro-IL-1β into mature IL-1β [18,19]. In this sense, it has been suggested that CD39 expression may contribute to dampening the ongoing inflammatory processes and/or rescue the cells from ATP-induced apoptosis/necrosis [20]. Ultimately, adenosine exerts potent anti-inflammatory effects. Recently, we have reported that purinergic signaling regulates the immune response to experimental *T. cruzi* infection. The temporal pharmacological inhibition of CD73 during the early acute phase of the infection induces microbicidal mechanisms, with the concomitant reduction in cardiac parasite load, improving the outcome of chronic cardiomyopathy [21].

The most common form of non-ischemic heart disease worldwide is represented by Chagas cardiomyopathy, which is caused by *T. cruzi* infection. It is estimated that around 8 million people are currently infected with this parasite, mostly in Latin America where the disease is endemic [22], but infection has expanded to non-endemic countries due to migratory movements [23]. During the acute phase, the heart is dramatically parasitized, thus myeloid cells are highly mobilized from the bloodstream into the myocardium to control parasite multiplication. Once there, monocytes differentiate into macrophages, which are in charge of inhibiting tissue parasite replication [24–26]. *In vitro* studies have revealed that *T. cruzi* infection stimulates M1 activation in cultured peritoneal macrophages [27] and that the modulation of macrophage activation may be an evasion mechanism to allow parasite persistence throughout arginase-I induction [28,29]. We have reported that cardiac arginase expression is higher and persists for a longer period in mice prone to infection [30]. Our and other reports [28,29] clearly indicate that arginase expression, which is induced in M2 macrophages, is associated with parasite growth and susceptibility to infection.

In the present work, we hypothesize that IL-6 critically directs innate immune response that mediates host survival after *T. cruzi* infection. Our results show, for the first time, that IL-6 is a key cytokine that drives monocyte recruitment and determines the establishment of the M2 cardiac macrophage profile during infection. This cytokine induced *in vivo* and *in vitro* expression of the ATP metabolic enzyme CD39 on macrophages, suggesting that IL-6 could promote a shift from an ATP driven pro-inflammatory environment to an anti-inflammatory milieu induced by adenosine. Considering that extracellular ATP is a common inflammasome-activating event [31,32] we focused on IL-1β production. We discovered that IL-6 regulates inflammasome activation and, consequently, IL-1β-induced NO production, and that excessive oxidative stress accounts for the increased mortality previously observed in infected IL-6-deficient (IL6KO) mice [10,11].

Considering that the signaling pathway of this cytokine is a therapeutic target in patients with different immune system-mediated diseases, our results provide the cellular and molecular basis for understanding why blocking IL-6 in certain clinical situations does not represent an effective treatment; instead triggering pro-inflammatory adverse events.

2. Materials and methods

2.1. Ethics statement

All animal experiments were approved by and conducted in accordance with guidelines of the Committee for Animal Care and Use of the CIBICI-CONICET (Approval Number 274/09) in strict accordance with the recommendation of the Guide to the Care and Use of Experimental Animals published by the Canadian Council on Animal Care.

Blood was drawn from control donors and chagasic patients using a protocol approved by the Comité Institucional de Ética de la Investigación en Salud del Adulto, Ministerio de Salud (Acta number 194/2014). All human studies were conducted according to the principles expressed in the Declaration of Helsinki. Written informed consent was obtained from all donors prior to their participation. *T. cruzi* infection was determined by a combination of indirect hemagglutination (IHA) and enzyme-linked immunosorbent assay (ELISA) performed in the laboratory of Hospital Nuestra Señora de la Misericordia (HNSM). Subject positive on these two tests were considered infected. Chronic chagasic patients ($n = 22$) were evaluated clinically and by electrocardiogram and chest X-ray. The uninfected control group ($n = 24$) consisted of age-matched individuals were serologically negative for *T. cruzi*. All donors with chronic or inflammatory pathology or erythrocyte sedimentation rate >30mm or white blood cells count <4000 or >10,000/mm^3 were excluded from the study.

2.2. Mice

Female IL6KO (B6.129S2-Il6^{tm1Kopf}/J) mice, female NLRP3KO (B6.129S6-Nlrp3^{tm1Bhk}/J) mice and female CD73KO (CD73KO-B6.129S1-Nt5e^{tm1Lft}/J) mice were purchased from The Jackson Laboratory (USA); female C57BL/6J mice were from Universidad Nacional de La Plata (Argentina). They were housed in the Animal Facility of the CIBICI-CONICET (OLAW-NIH assurance number A5802-01). Mice were anesthetized with isoflurane.

2.3. Parasites and experimental infection

Six to eight week-old mice were intraperitoneally infected with 1000 *T. cruzi* blood-derived trypomastigotes of Tulahuen strain. Only mice used in experiment of S6 Fig were infected with trypomastigotes of Y strain. Parasites were maintained by serial passages from mouse to mouse.

2.4. Heart histology, myocardial damage markers and cytokine levels

Hearts fixed in 10% buffered formalin were embedded in paraffin. Five-micron-thick sections were examined by light microscopy (Nikon Eclipse TE 2000 U) after hematoxylin/eosin or TUNEL staining. Plasma samples were sent to Biocon Laboratory, Córdoba-Argentina to measure total CK and CK-MB isozyme (BioSystems). The levels of cytokines in cardiac lysates, plasma or culture supernatants were quantified by ELISA assays. The total protein concentration of heart samples was determined by the Bradford method (Bio-Rad).

2.5. Heart-infiltrating cells isolation and flow cytometry

Cardiac leukocytes isolation was performed as previously described [33]. Briefly, hearts were perfused with PBS, and disaggregated mechanically and enzymatically with 0.2% trypsin solution (GIBCO). The digested tissue was pressed through a 70 μm cell strainer (BD Falcon), and the cells were isolated by 35% and 70% bilayer Percoll (GE

Healthcare) density gradient centrifugation. Viable cell numbers were determined by trypan blue exclusion using a Neubauer chamber. Cells were stained with the following antibodies: anti-mouse-APC-CD11b, PE-F4/80, APC-Cy7-CD86, PE-Cy7-CD206, FITC-Gr1, FITC-CD39 and PerCPCy5.5-CD73. Blood was treated with lysis buffer (GIBCO) and stained with the following antibodies: anti-mouse APC-CD11b, PECy7-Ly6C, APC-Cy7-Ly6G, Brilliant Violet 421-CCR2, PE-CCR5, PerCPCy5.5-CXCR2, CX3CR1 rabbit and anti-rabbit Alexa 488. Measure of NO-producing cells was determined with DAF-FM (Molecular Probes). Intracellular expression of iNOS Alexa 647 or Alexa 488 (BD Pharmingen) and arginase-I-FITC- (Santa Cruz) was determined using Foxp3 staining buffer (eBioscience). Stained samples were acquired using a FACS Canto II cytometer (Becton Dickinson) and the data were analyzed using FlowJo software (Tree Star). To all flow cytometric procedures isotype controls were used to discount nonspecific fluorescence.

2.6. IL-6 treatment in vivo

Human recombinant IL-6 (rhuIL-6) (Immunotools) was injected subcutaneously into IL6KO mice (500 ng/g of body weight) before infection. At 4 dpi circulating monocytes and heart-infiltrating cells were quantified.

2.7. Adoptive transfer experiment

At 2 dpi WT or IL6KO mice were intravenous transferred with 15×10^6 eFluor670 (eBioscience)-labeled WT spleen cells and 15×10^6 CFSE-labeled IL6KO spleen cells. After 48 h, heart, peripheral blood and spleen were obtained from WT and IL6KO recipient mice. Immune cells were isolated, stained and analyzed in the cytometer as described above.

2.8. Bone marrow derived macrophages (BMDM) differentiation and polarization

BMDM were obtained as previously described [34]. Cells were cultured in growth medium supplemented with 13% supernatant of the mouse L929 cell line (conditioned medium) for 7 days. For polarization 250,000 BMDM were stimulated with rmIL-4 (20 ng/mL), rmIL-6 (20 ng/mL) and rmIL-10 (10 ng/mL) (Immunotools, Biolegend and eBioscience) for 4 days. In other experiments, WT and NLRP3KO BMDM were stimulated with LPS (100 ng/mL) alone or with rmIL-6 (20 ng/mL) or anti-IL-1β (20 μg/mL) for 24 h or were infected at 1:1 parasite–host cell ratio for 3 h, and then stimulated or no with rmIL-6 (20 ng/mL) or anti-IL-1β or anti-IL-1β and anti-TNF (25 μg/mL) for 24 h. The cells were harvested and stained before measurement in the cytometer.

2.9. Parasite load

Genomic DNA was purified from infected hearts using TRIzol reagent following the manufacturer instructions. Satellite DNA from *T. cruzi* (GenBank AY520036) was quantified by real time PCR using specific Custom Taqman Gene Expression Assay (Applied Biosystems) and the primer and probe sequences described by Piron et al. [35]. Genomic DNA (1 μg) was amplified and expressed as arbitrary units compared to GAPDH expression.

2.10. Nitric oxide measurement

Nitrite/nitrate contained in plasma, heart lysates and culture supernatant were reduced to nitrite, which was measured spectrophotometrically by the Griess reaction. The total protein concentration of heart samples was determined by the Bradford method.

2.11. Detection of biomolecular oxidative damage

Malondialdehyde (MDA) level was measured by thiobarbituric acid (TBA) test, with separation and quantification of the MDA–TBA adducts by HPLC [36]. In brief, the proteins of heart lysates were precipitated with 5% trichloroacetic acid. The samples were treated with 0.25% TBA for 45 min at 90 °C, ice-cooled and analyzed by HPLC on a C18 column with UV detection (532 nm). The mobile phase used was 50 mM KH_2PO_4 (pH 6.0):methanol (65:35), at a flow rate of 2 mL/min. MDA levels were calculated from a calibration curve based on the acid hydrolysis of 1,1,3,3-tetraethoxypropane and the reaction with TBA.

2.12. Human cell culture

Erythrocytes from human peripheral blood were lysed with ACK lysing buffer, and monocytes were stained with anti-human CD14 PECy5, anti-human CD39 biotin and streptavidin APC and anti-human CD73 PE (eBioscience). To *in vitro* infection, 250 μL of peripheral blood was infected with 7500 trypomastigotes (Tulahuen strain) and stimulated with rhuIL-6 (20 ng/mL) or maintained in medium for 24 h. CD39 and CD73 expression and NO-producing leukocytes were determined by flow cytometry.

2.13. L-NAME treatment

IL6KO mice were infected and immediately treated with L-NAME (Sigma) in their drinking water for 1 week (50 mg/dL) to inhibit NO synthesis. Mice survival was followed up to 65 dpi.

2.14. Statistics

Statistical significance of comparisons of mean values was assessed by a two-tailed Student's *t*-test and, two-way ANOVA followed by Bonferroni's post-test and a Gehan-Breslow-Wilcoxon test using GraphPad software.

3. Results

3.1. IL-6 determines macrophage activation profile in infected heart tissue

We first comparatively analyzed the kinetics of macrophage subsets into the myocardium of infected IL6KO and WT mice. Single cell suspensions were analyzed for CD11b, F4/80 and Gr1 expression. In our model, the majority of F4/80 positive cells uniformly expressed CD11b, F4/80^{low} and were Gr1 negative. The infiltrating macrophages identified by F4/80^{low} expression [37], was further divided on M1 (CD11b + F4/80 + CD86 + CD206 −) and M2 (CD11b + F4/80 + CD86 − CD206 +) polarity (S1 Fig). Among the macrophages with M1 phenotype 86.13 ± 4.10% were positive for iNOS expression, whereas 88.17 ± 2.17% of macrophages with the M2 phenotype were positive for arginase-I expression (S2 Fig). In WT mice we found a prevalence of macrophages with M1 phenotype in the early days following infection (4 days post-infection [dpi]) over macrophages with M2 phenotype. Nevertheless, as soon as 7 dpi the M1 population diminished while the population of macrophages with the M2 phenotype strongly increased and remained steady up to 60 dpi (Fig. 1A). The same kinetics were observed in BALB/c mice [21], illustrating that alternatively activated macrophages comprise the main heart-infiltrating subset throughout the acute and chronic phase of the infection. In contrast, in IL6KO mice M2 macrophages never became the main population throughout the whole study period (Fig. 1B). In addition, in both animal strains M1 macrophage subset peak was associated with the highest rate of creatine kinase MB isozyme (CK-MB)/total CK, a specific biochemical index of cardiac damage (Fig. 1C). Strikingly, at 21 dpi the percentage of plasma CK-MB in surviving IL6KO mice diminished as a consequence of an excessive increase in total CK, suggesting generalized tissue

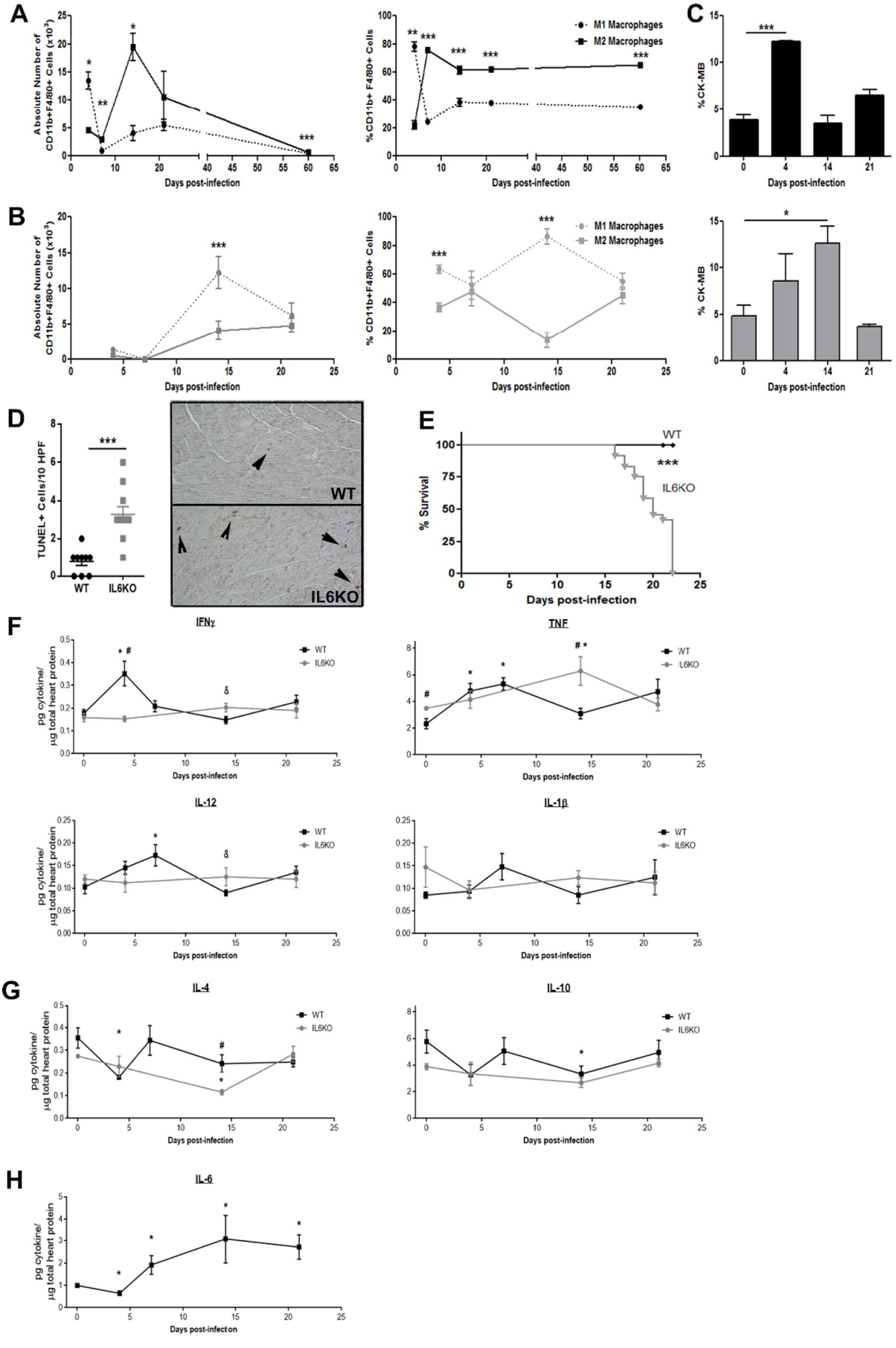
A
Absolute Number of CD11b+F4/80+ Cells (x10³)
Days post-infection
% CD11b+ F4/80+ Cells
M1 Macrophages
M2 Macrophages
C
% CK-MB
Days post-infection
B
Absolute Number of CD11b+F4/80+ Cells (x10³)
Days post-infection
% CD11b+F4/80+ Cells
M1 Macrophages
M2 Macrophages
% CK-MB
Days post-infection
D
TUNEL+ Cells/10 HPF
WT
IL6KO
WT
IL6KO
E
% Survival
WT
IL6KO
Days post-infection
F
IFNγ
pg cytokine/ µg total heart protein
WT
IL6KO
Days post-infecton
TNF
WT
L6KO
Days post-infection
IL-12
pg cytokine/ µg total heart protein
WT
IL6KO
Days post-infection
IL-1β
WT
IL6KO
Days post-infection
G
IL-4
pg cytokine/ µg total heart protein
WT
IL6KO
Days post-infection
IL-10
WT
IL6KO
Days post-infection
H
IL-6
pg cytokine/ µg total heart protein
Days post-infecton

damage or renal failure. In agreement with the progressive myocardial damage there were increased TUNEL-positive cells (Fig. 1D), and all IL6KO mice died between 16 and 22 dpi (Fig. 1E).

Concomitant with the predominance of M1 macrophages at 4 dpi, the levels of inflammatory cytokines IFNγ (M1 polarizing factor) and TNF significantly increased in WT mice (Fig. 1F). Furthermore, myocardial production of IL-4 (M2a polarizing cytokine) significantly diminished at this time point (Fig. 1G). On the other hand, concomitant with induction of M2 phenotype, the production of IFNγ and IL-12p70 significantly decreased at 14 dpi compared to the amounts observed at 4 dpi. Together, these results demonstrated that the changes in pro- and anti-inflammatory cytokines approximately follow the kinetics of cardiac macrophages profiles. However, considering the poor regenerative capacity of cardiomyocytes, it is plausible to think that a highly polarized pro-inflammatory microenvironment would be catastrophic for the heart. In this way of thinking, it has been demonstrated that Toll like receptor activation (specifically TLR9) in cardiac cells does not follow the canonical inflammatory signaling of immune cells [38]. Moreover, we have reported that infection of cardiomyocytes with *T. cruzi* leads to a selective production of IL-6 (but not IL-1β, TNF, IL-12 and IL-17 pro-inflammatory cytokines) [8]. In both experimental models, the activation of TLRs triggers mechanisms of cellular protection in cardiomyocytes clearly illustrating that cardiac tissue increase the stress tolerance whereas immune cells induce inflammation upon TLR ligand stimulation.

Notably, levels of IL-6 diminished at 4 dpi but increased steadily from 7 dpi, following the kinetics observed for M2 macrophages (Fig. 1H). Furthermore, in the IL-6-deficient myocardium, TNF production increased at 14 dpi, while microbicidal IFNγ remained unmodified at all time-points studied. Moreover, the levels of IL-4 and IL-10 substantially dropped at this time point, coincident with the dominance of the M1 phenotype (Fig. 1F and G). These results strongly suggest that IL-6 may be a keystone cytokine for determining the activation profile of macrophages in infected heart tissue.

In both animal strains, cardiac MCP-1 levels increased throughout the infection and no changes were detected in IL-17 at all-time points analyzed (S3 Fig).

3.2. IL-6 is a critical mediator of leukocyte influx to infected myocardium

Considering the significantly lower number of macrophages infiltrating the infected IL6KO myocardium observed by FACS (Fig. 1) and by histological studies (Fig. 2A–G), we wondered whether myocardial IL-6 production triggered the recruitment of immune cells into infected hearts. Thus, we performed adoptive transfer experiments with a scheme involving one injection of an equal number of WT and IL6KO spleen cells. Total heart-infiltrating cells in WT recipient were higher than in IL6KO recipient (Fig. 2H). However, the rate of injected cells in the peripheral blood was the same in both recipients (Fig. 2I), suggesting that both cell populations were equally competent in reaching circulation. Nevertheless, while an equal frequency of injected cells arrived at the WT myocardium, a significantly lower percentage of total adoptively transferred IL-6-deficient cells compared to WT cells reached the IL6KO myocardium (Fig. 2J). Furthermore, the frequency of injected IL6KO F4/80+ cells that migrated to the myocardium was significantly lower than injected WT F4/80+ cells in cytokine-deficient heart tissue (Fig. 2K). In addition, the percentage of total and F4/80+ fluorescent IL-6-deficient cells was significantly increased in the spleen of IL6KO mice (Fig. 2L and M). In agreement with these results, the frequency of circulating CX3CR1+ inflammatory monocytes was lower in IL6KO mice in comparison with WT mice (S4 Fig). To confirm the role of IL-6 in leukocyte influx, IL6KO animals were subjected to one subcutaneous dose of rhuIL-6 prior to infection. While treated mice presented a decrease in the percentage of circulating inflammatory monocytes (Fig. 3A), heart-infiltrating cells significantly increased (Fig. 3B) with considerably greater influx of macrophages (Fig. 3C). Thus, the rhuIL-6-treated animals presented an increased number of cardiac M1 and M2 macrophages (Fig. 3D and E). These results corroborate that IL-6 plays a critical role in the recruitment of cells to infected cardiac tissue.

3.3. IL-6 promotes alternative activation of macrophages

Taking into account that IL6KO infiltrating macrophages never developed a predominant M2 phenotype, we evaluated whether this cytokine had a role in promoting an alternative activation profile *in vitro*. The incubation with rmIL-6 increased the percentage of BMDM from WT polarized to M2 profile and diminished the frequency of M1 macrophages (Fig. 4A and B), decreasing the release of TNF and increasing the levels of IL-4 in the culture supernatants (Fig. 4C). Among the possible mechanisms involved in IL-6-induced M2 profile, ATP catabolic machinery could have a role. In fact, the rmIL-6 stimulation significantly increased the percentage of CD39+ BMDM from WT or IL6KO (Fig. 4D), while CD73 expression did not change (Fig. 4E). In agreement, the percentage of infiltrating leukocytes expressing CD39 was higher in WT than in IL6KO myocardium (Fig. 4F). Moreover, the stimulation of peripheral blood from chagasic patients with rhuIL-6, increased the percentage of CD39+ monocytes, but did not modify CD73 expression in monocytes (Fig. 4G). Nevertheless, while the percentage of CD39+ circulating leukocytes did not show significant differences, the percentage of CD73+ leukocytes were significantly lower in seropositive patients compared with control donors (Fig. 4H). Consistent with our previous studies [21], we observed that rmIL-6 failed to increase the percentage of M2 BMDM from CD73KO mice (Fig. 4I). The results suggest that IL-6 could trigger a shift from an ATP-driven pro-inflammatory environment to an anti-inflammatory milieu induced by adenosine.

3.4. Infected IL-6-deficient mice show increased plasma levels of IL-1β and higher cardiac and systemic levels of nitric oxide

The decreased myocarditis observed in IL6KO mice, as evaluated by the number of cardiac-infiltrating cells, suggested a more permissive environment for parasite development in the myocardium. However, cardiac parasite burden and parasitemia were significantly lower than in WT animals (Fig. 5). This led us to explore inflammatory mediators with microbicidal activity in IL6KO mice. While no changes were observed in plasma levels of most tested cytokines between both mouse strains (S5 Fig), IL6KO mice showed a progressive increase in IL-1β levels throughout the kinetic studies (Fig. 6A) and a strong increase in plasma NO levels compared to WT animals at 4 and 21 dpi (Fig. 6B). Furthermore, cardiac NO levels peaked in WT and IL-6-deficient mice at 4 dpi, but then, while them diminished in WT throughout the infection, in IL6KO mice remained steadily (Fig. 6C). Similar results were obtained in mice infected with the Y strain (S6 Fig). In accordance, deficient animals presented a significantly increased percentage of circulating inflammatory monocytes at all time-points studied (Fig. 6D). Furthermore, the percentage of iNOS-expressing monocytes (Fig. 6E) and cardiac macrophages (Fig. 6F) were significantly higher in IL6KO mice in comparison with WT mice. In accordance, higher levels of

Fig. 1. IL-6 determines macrophage activation profile in infected heart tissue. Absolute number and relative percentage of macrophages with M1 and M2 phenotype detected in WT (A) and IL6KO (B) infected hearts. Percentages are expressed as the relationship between both single positive populations. Relative percentage of plasma CK-MB activity with respect to total CK activity in WT (black bars) and IL6KO (grey bars) mice (C). At 21 dpi the percentages of CK-MB were determined in the plasma of surviving IL6KO mice. Number of dead cells (Left) quantified in myocardial slides from 21 dpi and representative images of TUNEL staining of WT (Top-Right) and IL6KO (Bottom-Right) (D). Survival of IL6KO and WT infected mice (Gehan Breslow Wilcoxon test) (E). Levels of cardiac M1 (F) and M2 (G) related cytokines and IL-6 (H) in relation to total heart protein in WT (black lines) and IL6KO (grey lines) mice. * $p < 0.05$ *vs* the uninfected group, & $p < 0.05$ 4 dpi *vs* 14 dpi, # $p < 0.05$ WT *vs* IL6KO. Results are expressed as mean ± SEM ($n = 6$) of at least three independent experiments. *$p < 0.05$; **$p < 0.01$; ***$p < 0.001$.

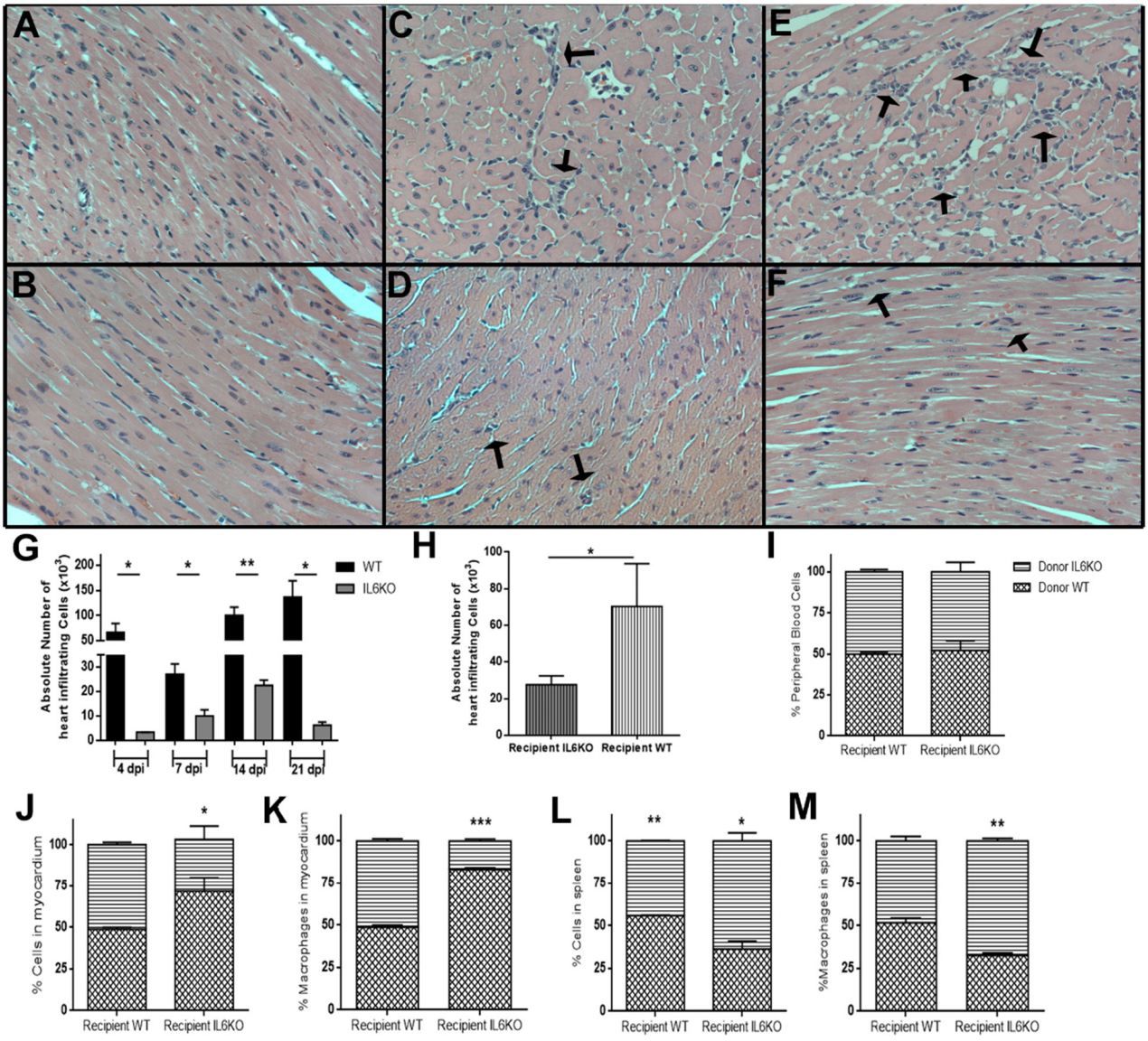

Fig. 2. IL-6 is a critical mediator of leukocyte influx to infected myocardium. Representative histological sections of uninfected, 14 and 21 dpi heart tissue from WT (A, C and E, respectively) and IL6KO (B, D and F, respectively) mice stained with hematoxylin and eosin. 200×. Arrows: inflammatory foci. Number of total infiltrating cells in myocardium counted in a Neubauer chamber (G). Equal number of e-Fluor670-labeled WT and CFSE-labeled IL6KO spleen cells were transferred into WT or IL6KO mice at 2 dpi. After 48 h the absolute number of total heart-infiltrating cells was counted (H). The relative percentage of e-Fluor670-WT cells (checkered bars) and CFSE-IL6KO cells (striped bars) with respect to total fluorescent cells was determined in peripheral blood (I), myocardium (J) and spleen (L). The relative percentage of transferred F4/80+ cells was quantified in myocardium (K) and spleen (M). Results are expressed as mean ± SEM ($n = 5$) of two independent experiments. $^{*}p < 0.05$, $^{**}p < 0.01$, $^{***}p < 0.001$ comparing fluorescent WT cells with fluorescent IL6KO cells in the same recipient.

cardiac MDA (oxidative damage marker) were observed in IL6KO mice compared to WT mice (Fig. 6G). The increased oxidative damage could be responsible for the higher mortality observed in the absence of IL-6.

3.5. IL-6 regulates nitric oxide production through IL-1β modulation

Next, we wonder to determine whether IL-6 was capable of inhibiting NO production. In fact, rmIL-6 blunted LPS-induced NO production in BMDM (Fig. 7A), as well as the NO produced by infected WT BMDM (Fig. 7D). Moreover, when cells were stimulated with LPS + anti-IL-1β, the diminution of NO-producing cells as well as the intracellular levels of NO, were similar to those observed in LPS + rmIL-6-treated cells. No differences were observed when macrophages from animals deficient in NLRP3, the most clinically relevant inflammasome [39], were cultured with LPS alone or in combination with rmIL-6 (Fig. 7B). In accordance, WT macrophages produced significantly higher levels of NO compared to NLRP3KO macrophages (Fig. 7C). Moreover, rmIL-6 and anti-IL-1β blunted *T. cruzi*-induced iNOS expression in BMDM (Fig. 7E). To confirm whether IL-6 regulates IL-1β and NO *in vivo*, we treated IL6KO mice with a subcutaneous injection of rhuIL-6. The treatment significantly decreased systemic levels of NO and IL-1β (Fig. 8A), confirming that IL-6 inhibits both inflammatory mediators. Interestingly, rhuIL-6 stimulation also significantly diminished the percentage of *in vitro* infected NO-producing human monocytes from chagasic patients and control donors (Fig. 7F), demonstrating that the anti-oxidant effect of IL-6 is also exerted in human cells.

3.6. Inhibition of nitric oxide production increase the survival of IL-6-deficient mice

To evaluate whether the inhibition of NO production could rescue IL-6-deficient mice from death, we administrated L-NAME (analog of arginine) in the drinking water of IL6KO infected mice for one week since the day of the infection [40]. The survival rate detected at 22 dpi was 100% with a 29% of survivors even at 65 dpi (Fig. 8B).

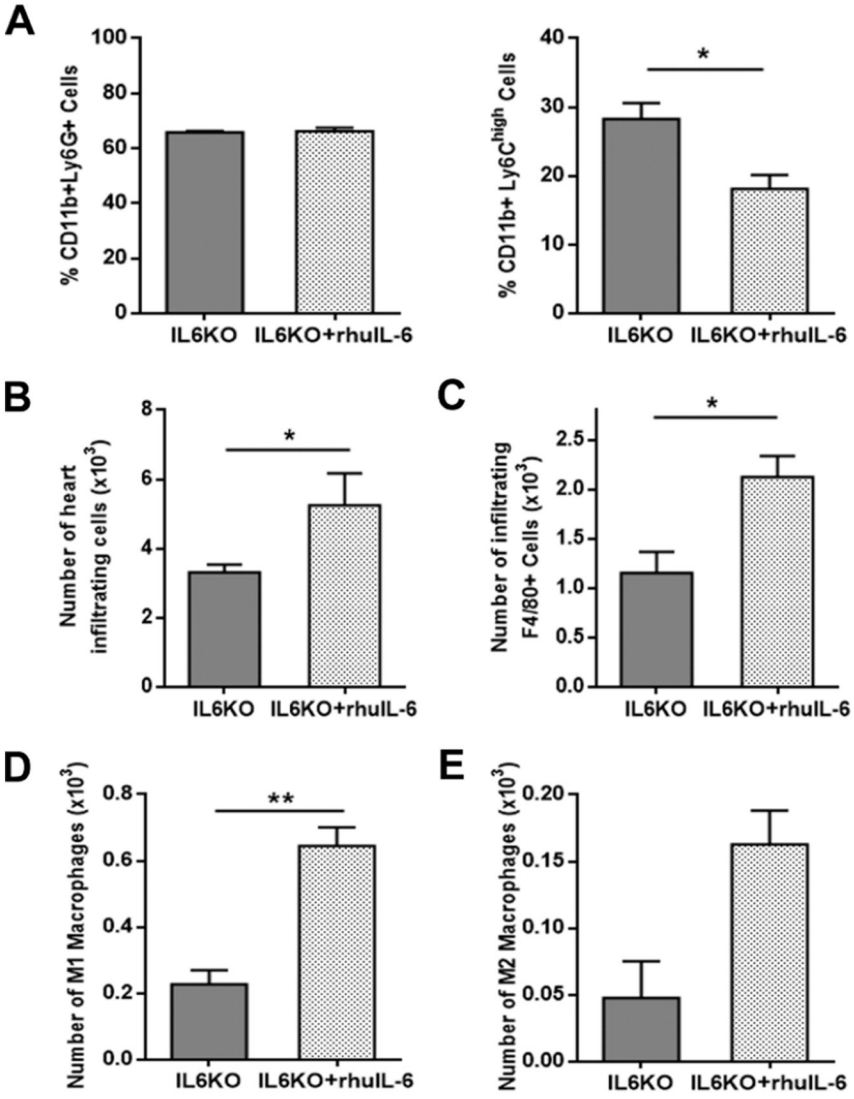

Fig. 3. IL-6 induces macrophage recruitment to infected heart tissue. IL6KO animals were treated with one subcutaneous injection of rhuIL-6 before infection (IL6KO + rhuIL-6) and at 4 dpi (A) CD11b+Ly6G+ and CD11b+Ly6C^{high} subpopulations were evaluated in peripheral blood of IL6KO (grey bars) and IL6KO treated animals (dotted bars). Absolute number of total infiltrating cells (B), CD11b+F4/80+ cells (C), M1 (CD11b+F4/80+CD86+CD206−) macrophages (D) and M2 (CD11b+F4/80+CD86−CD206+) macrophages (E) in the myocardium of IL6KO and IL6KO + rhuIL-6 mice. Results are expressed as mean ± SEM ($n = 4$) of two independent experiments. $^{*}p < 0.05$, $^{**}p < 0.01$, $^{***}p < 0.001$.

4. Discussion

At the outset of the present study, we had limited knowledge of the factors that drive host cardiac macrophage response to fight the intracellular parasite *T. cruzi*. As a result of the evaluation of monocyte/macrophage profile kinetics and *in vitro* experiments, we are now able to place IL-6 as the key player in the acquisition of macrophage activation state and macrophage influx into the infected myocardium.

In line with our previous reports indicating that IL-6 induces myeloid-derived suppressor cells recruitment during infection [11], we observed that IL-6 was also required for leukocyte migration to the infected myocardium independently of the cellular source of the cytokine. While infected IL6KO mice showed a marked reduction in cardiac inflammatory infiltration in comparison with infected WT mice, rhuIL-6 significantly increased the fate of infiltrating cells, particularly macrophages.

IL-6 deficiency failed to induce a predominant M2 phenotype, concomitant with lower parasite burden but also with enhanced mortality. Supporting these results, *in vitro* treatment with bioactive recombinant IL-6 promoted the alternative activation of BMDM. Together, these results demonstrate that IL-6 is a critical instigator of the M2 polarization of macrophages and has an assigned role in the modulation of cardiac response to infection. These findings may seem unexpected, given the general assumption that IL-6 acts as a pro-inflammatory cytokine [41–44]. In agreement with our results, however, it was recently reported that IL-6 signaling drives macrophage polarization toward alternative activation in the setting of LPS-induced endotoxemia and diet-induced obesity [45]. In this sense, it has been earlier reported that IL-6 plays a protective role against death in a murine model of septic shock. In that study the authors demonstrated *in vivo* antagonistic activities of IL-6 and TNF [46], thereby confirming a previous report in which IL-6 inhibited TNF production by LPS-stimulated human monocytes and *in vivo* murine model [47]. In accordance, in our work IL-6 significantly reduced the levels of TNF secreted by BMDM. Nevertheless, plasma levels of TNF do not elicited changes during the infection of IL6KO mice, suggesting that in the setting of *T. cruzi* infection IL-6 does not exert its anti-inflammatory effects through the inhibition of this potent inflammatory cytokine.

The novel finding that inflammation-induced IL-6 acts as a rapid brake on pro-inflammatory macrophage effector functions was further revealed by other recent reports. In a murine model of nephrotoxic nephritis IL-6 blockage significantly and selectively enhances renal

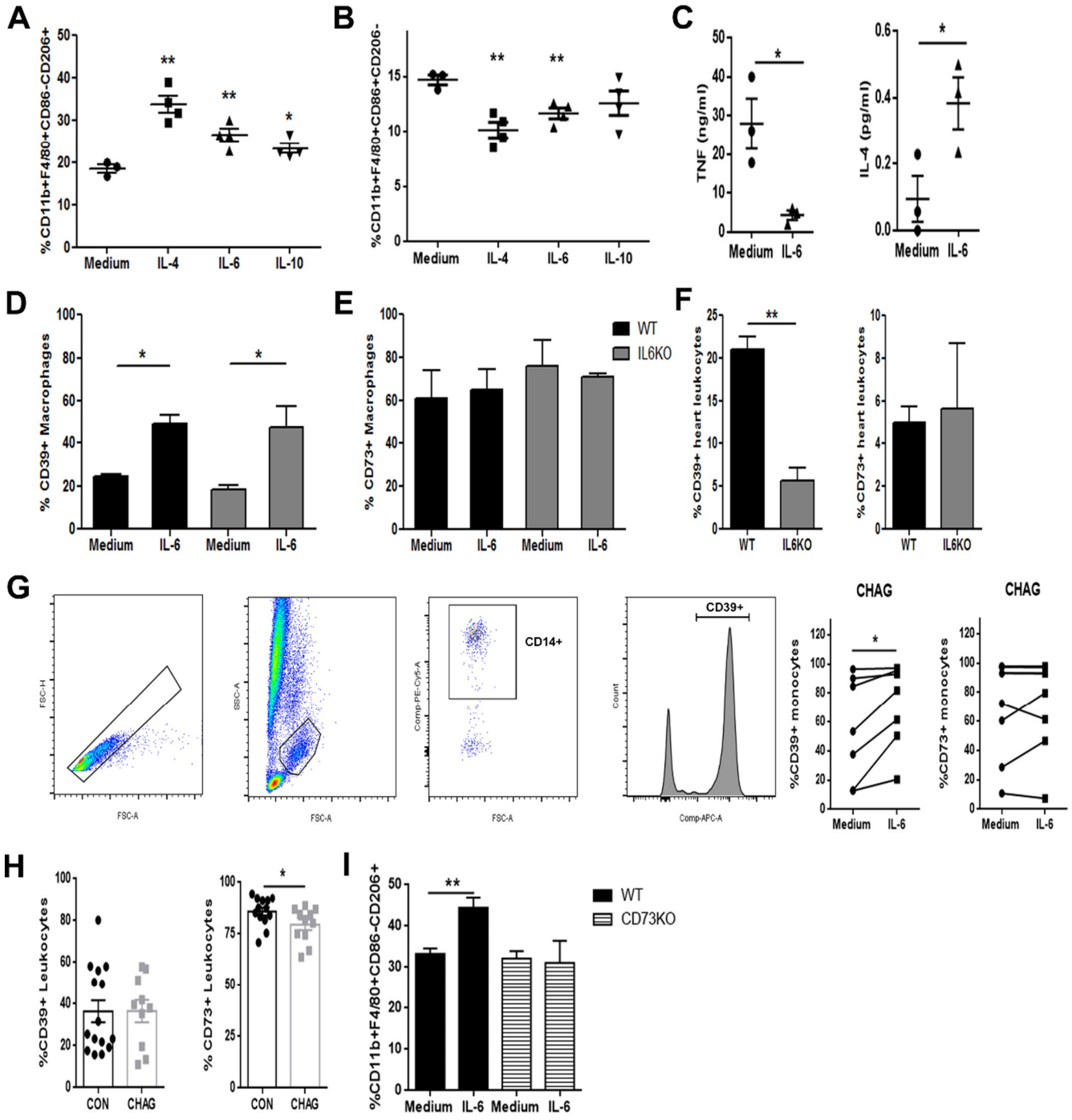

Fig. 4. IL-6 promotes alternative activation of macrophages. Percentage of M2 macrophages (A) and percentage of M1 macrophages (B) WT BMDM cultured with rmIL-4 or rmIL-6 or rmIL-10 or maintained in medium alone for 96 h. TNF and IL-4 levels from culture supernatants of WT BMDM stimulated with rmIL-6 or maintained in medium alone (C). Frequency of CD39+ (D) and CD73+ (E) BMDM cultured with rmIL-6 or maintained in medium. Percentage of CD39+ and CD73+ heart-infiltrating leukocytes in WT (black bars) and IL6KO (grey bars) mice at 21 dpi (F). Gate strategy to evaluate CD39 expression in monocytes and frequency of CD39+ and CD73+ monocytes from chagasic patients ($n = 10$) after rhuIL-6 stimulation *versus* unstimulated cells (G). Percentage of CD39+ and CD73+ circulating leukocytes from seropositive ($n = 13$) and seronegative ($n = 15$) individuals (H). Percentage of M2 macrophages from WT and CD73KO BMDM cultured with rmIL-6 (I). Results are expressed as mean ± SEM ($n = 6$) of at least three independent experiments performed in quadruplicate $^{*}p < 0.05$, $^{**}p < 0.01$, $^{***}p < 0.001$.

inflammatory macrophage absolute number while mannose receptor-positive M2 macrophages are reduced, indicating a switch toward a predominance of the M1 subtype. Therefore, IL-6 depletion is associated with an aggravation of nephritis [48]. IL-6-expressing macrophages were also associated to protection from neuroinflammation induced by immunization with a myelin antigen, suggesting that IL-6 anti-inflammatory properties also prevail in the central nervous system [49]. These observations have great implications because IL-6 anti-inflammatory activity might constitute a common mechanism protecting the organism from overshooting immune responses during acute inflammatory diseases. Nevertheless, IL-6 has been also implicated in cancer. Using a lung cancer mouse model, Caetano and colleagues have demonstrated that anti-IL-6 treatment significantly inhibits lung tumorigenesis that is correlated with a shift in the lung microenvironment toward a less suppressive antitumor myeloid phenotype [50].

One potential regulatory system that could have a role in the IL-6-induced M2 profile is the extracellular levels of adenosine. After infection, the influx of immune cells consumes large quantities of oxygen, and

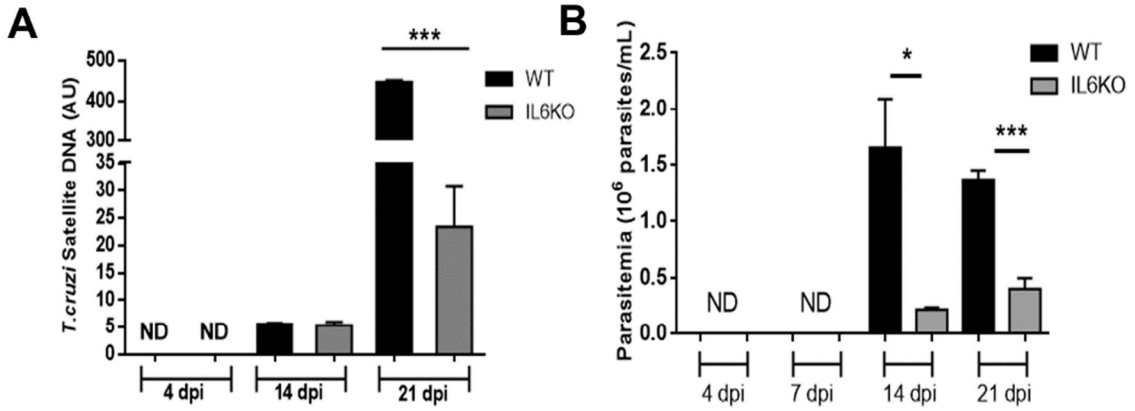

Fig. 5. IL-6-deficient mice present low parasitemia and cardiac parasite burden. Relative amounts of *T. cruzi* satellite DNA in the hearts of WT and IL6KO mice determined by real-time PCR (A). Murine GAPDH was used for normalization. Parasitemia (B). Results are expressed as mean ± SEM ($n = 6$) of at least three independent experiments. $^{*}p < 0.05$, $^{***}p < 0.001$.

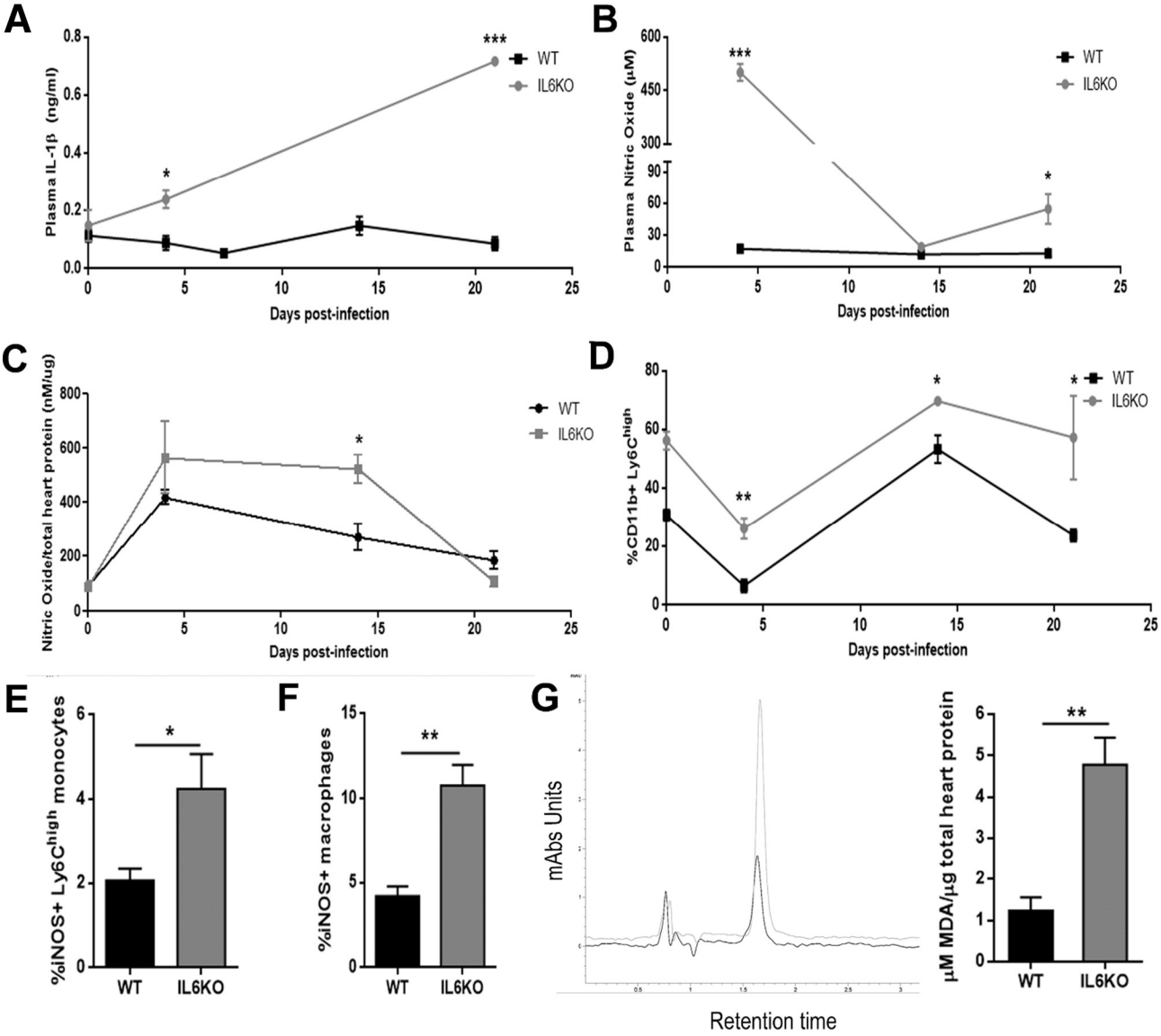

Fig. 6. Infected IL-6-deficient mice show increased plasma levels of IL-1β and higher cardiac and systemic levels of nitric oxide. Plasma levels of IL-1β (A) and NO (B) were measured by ELISA and Griess reagent, respectively, in WT and IL6KO animals. Cardiac levels of NO (C) in WT and IL6KO mice. $^{*}p < 0.05$ WT *versus* IL6KO. CD11b + Ly6C^{high} subpopulation in peripheral blood of WT (black lines) and IL6KO (grey lines) mice (D). Frequency of iNOS + inflammatory monocytes in peripheral blood and (F) iNOS + cardiac macrophages from WT and IL6KO at 4 dpi (E). Representative chromatograms evidencing cardiac MDA levels determined by HPLC in heart lysates of WT (black bars) and IL6KO (grey bars) mice at 14 dpi (G). Results are expressed as mean ± SEM ($n = 5$) of at least three independent experiments. $^{*}p < 0.05$, $^{**}p < 0.01$, $^{***}p < 0.001$.

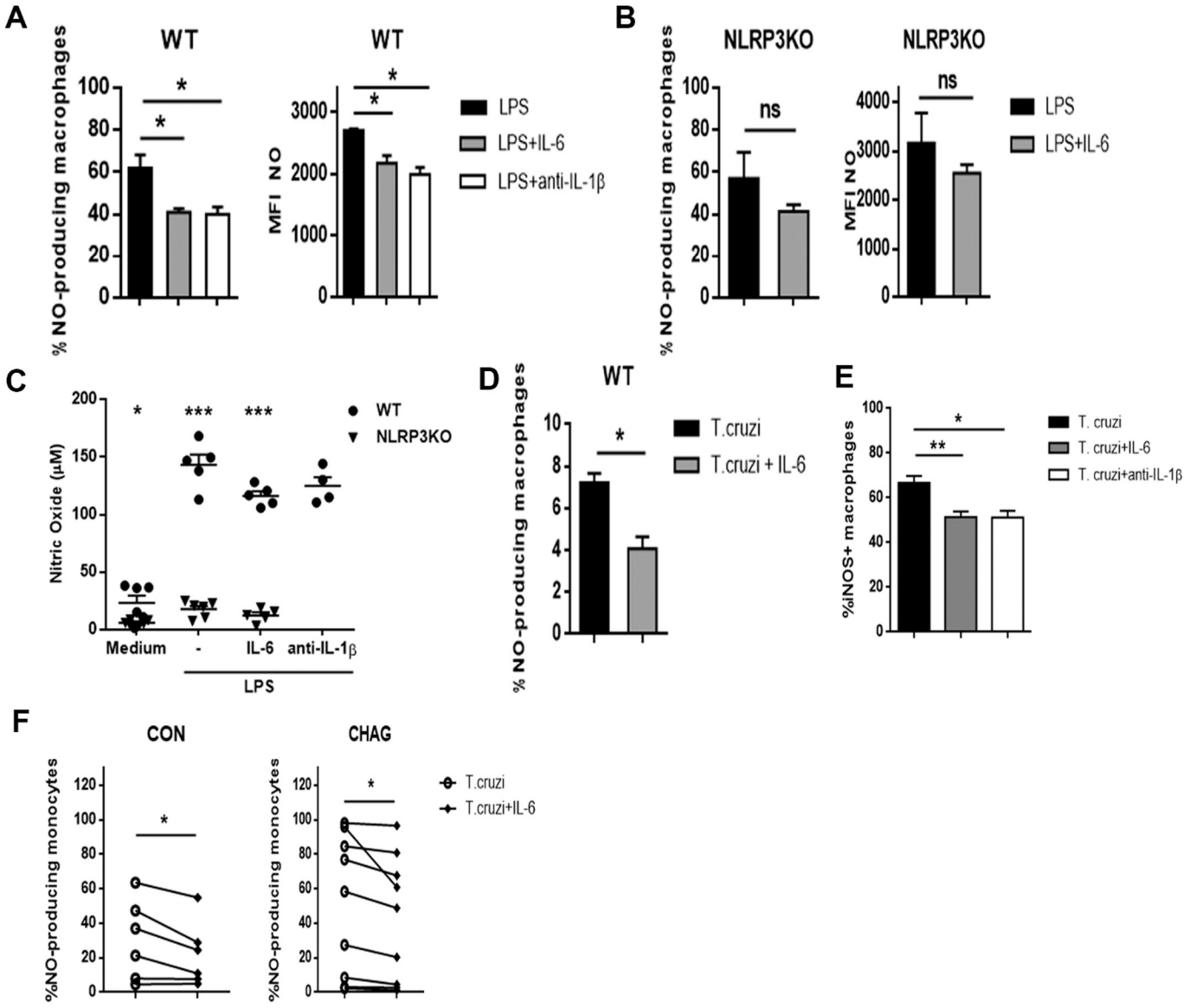

Fig. 7. IL-6 regulates nitric oxide production through IL-1β modulation. BMDM from WT (A) and NLRP3KO (B) mice were cultured with LPS alone or in combination with rmIL-6 or in combination with anti-IL-1β for 24 h. The percentage of NO-producing macrophages and the mean fluorescence intensity (MFI) of NO production were measured with the NO-specific probe DAF-FM. Levels of NO from culture supernatants of WT BMDM (black circle) are compared with the levels of NO in NLRP3KO BMDM supernatants (black triangle) BMDM measured with Griess reagent (C). The results are expressed as mean ± SEM of at least two independent experiments performed in quadruplicate. Percentage of NO-producing *in vitro T. cruzi* infected BMDM culture with rmIL-6 or maintained in medium (D). Frequency of iNOS+ macrophages after *in vitro T. cruzi* infection alone or in combination with rmIL-6 or with anti-IL-1β (E). Percentage of NO-producing monocytes/macrophages from human peripheral blood infected *in vitro* and stimulated with rhuIL-6 or maintained in medium alone (F). Results were obtained from three independent donors. $^{*}p < 0.05$, $^{**}p < 0.01$, $^{***}p < 0.001$.

ischemic cells rapidly respond to the hypoxic and inflammatory environment by releasing ATP [51,52]. Once released, ATP is converted to AMP and then to adenosine by CD39 and CD73, respectively. Adenosine affects macrophage function through several diverse mechanism [17,53,54], in particular inducing cardiac macrophages to adopt an M2-biased phenotype and driving the timely resolution of inflammation [52]. In this study, we found that IL-6 significantly increased the ATP machinery expression in murine and human cells. In pathological conditions, high levels of ATP activate the inflammasome that processes pro-IL-1β into mature IL-1β in macrophages [55]. In this sense, as a consequence of the lower expression of ATP metabolic machinery, the IL-6 deficiency could induce ATP accumulation and inflammasome activation that lead to increased IL-1β production. Activation of inflammasome also triggers pyroptosis, a highly inflammatory form of programmed cell death. In agreement, increased cell death rates occurred within infected IL6KO myocardium

We identified in infected IL6KO mice a sustained rise in plasma levels of IL-1β concomitant with a strong increase in the levels of plasma and cardiac NO that was also associated with an increased percentage of inflammatory monocytes, a population that rapidly responds to microbial stimuli by secreting NO [56]. Our results point to a critical role for IL-6 in the negative regulation of NO production. Supporting our results, it has been reported that nitrites production is blocked by IL-6 treatment of thioglycollate-elicited murine peritoneal macrophages stimulated with IFN-γ [57]. Thus, the high plasma NO output in addition to the increased amount of circulating inflammatory monocytes account for the lower parasite load detected in IL6KO mice. In accordance with a previous report [10], we detected no changes in cardiac and plasma

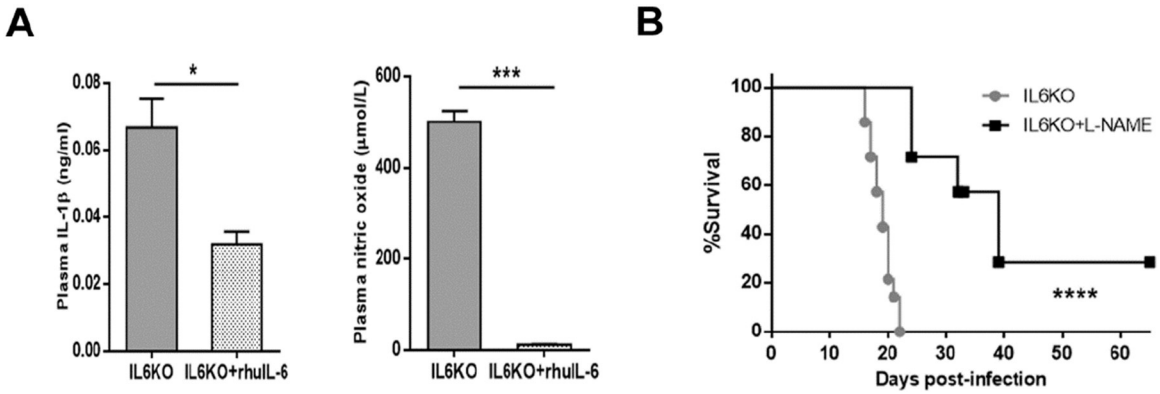

Fig. 8. IL-6 inhibited lethal nitric oxide and IL-1β *in vivo*. Plasma levels of IL-1β and NO from IL6KO and IL6KO + rhuIL-6 animals at 4 dpi (A). Survival rate of IL6KO and L-NAME treated IL6KO (IL6KO + L-NAME) infected mice (Gehan-Breslow-Wilcoxon test) (B). Results are expressed as mean ± SEM ($n = 5$) of at least two independent experiments. $^{*}p < 0.05$, $^{**}p < 0.01$, $^{***}p < 0.001$.

levels of IFNγ production in these infected mice, suggesting that other mediators could be responsible for uncontrolled levels of NO. In fact, *in vitro* and *in vivo* strategies demonstrated that IL-6 regulates NO production, at least in part, by controlling IL-1β levels. The biological relevance of these mechanisms was clearly illustrated by excessive myocardial oxidative stress observed and the improvement of survival of infected IL6KO mice treated with a NO inhibitor.

In agreement with our results, Gao and Pereira previously found increased mortality of IL6KO mice infected with *T. cruzi*-Tulahuen strain compared to infected B6-WT mice (the same mouse and parasite strains employed in our model) [10]. However, in contrast with our results they found an increase in parasitemia. A possible explanation for the increment in parasitemia could be that the inoculum was three-fold bigger and that the infection was performed by a subcutaneous pathway, which is more virulent than the intraperitoneal one [58]. This is illustrated by the fact that WT mice, in Gao's work, also succumbed to infection during the acute phase. In accordance with our results, however, the authors found unexpectedly similar serum IFNγ levels between infected WT mice and infected IL6KO mice. In light of our results, it is plausible to think that the higher levels of NO observed in IL6KO mice at the initiation phase of the immune response inhibit the production of IFNγ and in consequence its levels remained unaffected. In this sense, a strong immune regulatory role for NO has long been recognized [59,60]. Seminal experiments have revealed that NO selectively inhibits the expansion of Th1 cells by a negative feedback mechanism [61,62].

Studying the etipathological mechanism involved in human Chagas disease we have recently reported that IL-1β secretion is significantly diminished in infected human peripheral blood mononuclear cells cultured with rIL-6. Furthermore, we demonstrated that IL-6 regulates oxidative stress through IL-1β inhibition since the percentage of NO-producing monocytes significantly diminished when both cytokines (IL-1β plus IL-6) are blocked compared with the inhibition of IL-6 alone. These anti-oxidant properties allow IL-6 to revert the increased nitration observed in CD8 + cells from Chagas patients and improve the cytotoxic T cell functionality [63].

IL-6 is considered as a keystone cytokine that supports several immune system-mediated diseases and, in consequence, targeting IL-6 offers an opportunity for remission [64]. Current IL-6-targeted therapies display robust safety profiles; however, they show strong efficacy in some clinical indications but weak in others. Many of the diseases in which inhibition of IL-6 is clinically beneficial are often associated with dysregulated adaptive, but not innate immunity [65]. Our results provide the cellular and molecular basis for understanding why blocking IL-6 in certain clinical situations does not represent an effective treatment, instead triggering pro-inflammatory adverse events. This will open new avenues toward designing improved intervention strategies, including patient stratification, increasing the opportunities for remission.

5. Conclusion

Summing up, the anti-inflammatory action of IL-6 appears to be central to control local and systemic oxidative stress, promoting cell survival and protecting the host against death. Although cardiac innate immune response against this parasite has a key role in determining the outcome of the infection, it is plausible that additional effector cell populations within the heart or in other tissues could have a role.

Authorship

Contribution: Conceived and designed the experiments: LMS NEP MPA. Performed the experiments: LMS NEP LMV NE MGT MPA. Analyzed the data: LMS NEP NE MPA. Patients handling and human samples: LMV ARM. Wrote the paper: LMS MPA.

Transparency document

The Transparency document associated with this article can be found, in online version.

Acknowledgments

This work was funded by Secretaría de Ciencia y Tecnología, Universidad Nacional de Córdoba (05/C642), Agencia Nacional de Promoción Científica y Tecnológica (ANPCyT) (PICT 2013-2885) Fondo para la Investigación Científica y Tecnológica (PICT 2013-2885), Consejo Nacional de Investigaciones Científicas y Técnicas (CONICET) (PIP 11220120100620) and by Ministerio de Ciencia y Tecnología, Gobierno de la Provincia de Córdoba, Secretaría de Ciencia y Tecnología (1143/10). M.P.A. and M.G.T. are members of the scientific career from the Consejo Nacional de Investigaciones Científicas y Técnicas de la República Argentina (CONICET). L.M.S. and N.E.P. thank CONICET for the fellowships granted; L.M.V. and N.E. thank fellowship granted from Fundación Florencio Fiorini and ANPCyT-FONCyT respectively. We are grateful to Dr. Adriana Gruppi for the Y strain trypomastigotes donation and to Dr. F. Cerban, Dr. C. Stempin and R.C. Cano for discussion and critical reading of the manuscript. We thank Alejandra Romero, Pilar Crespo, Paula Abadie, Cecilia Sampedro, Carlos Mas, Belkys Maletto,

Yamile Ana, David Rojas Marquez, Jimena Tosello-Boari, Carolina Florit, Victoria Blanco, Diego Lutti and Fabricio Navarro for their skillful technical assistance.

Appendix A. Supplementary data

Supplementary data to this article can be found online at http://dx.doi.org/10.1016/j.bbadis.2017.01.006.

References

[1] M. Rattazzi, M. Puato, E. Faggin, B. Bertipaglia, A. Zambon, P. Pauletto, C-reactive protein and interleukin-6 in vascular disease: culprits or passive bystanders? J. Hypertens. 21 (2003) 1787–1803.
[2] T. Tsutamoto, T. Hisanaga, A. Wada, K. Maeda, M. Ohnishi, D. Fukai, N. Mabuchi, M. Sawaki, M. Kinoshita, Interleukin-6 spillover in the peripheral circulation increases with the severity of heart failure, and the high plasma level of interleukin-6 is an important prognostic predictor in patients with congestive heart failure, J. Am. Coll. Cardiol. 31 (1998) 391–398.
[3] M. Hogye, Y. Mandi, M. Csanady, R. Sepp, K. Buzas, Comparison of circulating levels of interleukin-6 and tumor necrosis factor-alpha in hypertrophic cardiomyopathy and in idiopathic dilated cardiomyopathy, Am. J. Cardiol. 94 (2004) 249–251.
[4] E. Roig, J. Orus, C. Pare, M. Azqueta, X. Filella, F. Perez-Villa, M. Heras, G. Sanz, Serum interleukin-6 in congestive heart failure secondary to idiopathic dilated cardiomyopathy, Am. J. Cardiol. 82 (1998) 688–690 (A688).
[5] K. Maeda, T. Tsutamoto, A. Wada, N. Mabuchi, M. Hayashi, T. Tsutsui, M. Ohnishi, M. Sawaki, M. Fujii, T. Matsumoto, M. Kinoshita, High levels of plasma brain natriuretic peptide and interleukin-6 after optimized treatment for heart failure are independent risk factors for morbidity and mortality in patients with congestive heart failure, J. Am. Coll. Cardiol. 36 (2000) 1587–1593.
[6] J. Orus, E. Roig, F. Perez-Villa, C. Pare, M. Azqueta, X. Filella, M. Heras, G. Sanz, Prognostic value of serum cytokines in patients with congestive heart failure, J. Heart Lung Transplant. 19 (2000) 419–425.
[7] E.J. Birks, N. Latif, V. Owen, C. Bowles, L.E. Felkin, A.J. Mullen, A. Khaghani, P.J. Barton, J.M. Polak, J.R. Pepper, N.R. Banner, M.H. Yacoub, Quantitative myocardial cytokine expression and activation of the apoptotic pathway in patients who require left ventricular assist devices, Circulation 104 (2001) I233–I240.
[8] N.E. Ponce, R.C. Cano, E.A. Carrera-Silva, A.P. Lima, S. Gea, M.P. Aoki, Toll-like receptor-2 and interleukin-6 mediate cardiomyocyte protection from apoptosis during *Trypanosoma cruzi* murine infection, Med. Microbiol. Immunol. 201 (2012) 145–155.
[9] N.E. Ponce, E.A. Carrera-Silva, A.V. Pellegrini, S.I. Cazorla, E.L. Malchiodi, A.P. Lima, S. Gea, M.P. Aoki, *Trypanosoma cruzi*, the causative agent of Chagas disease, modulates interleukin-6-induced STAT3 phosphorylation via gp130 cleavage in different host cells, Biochim. Biophys. Acta 1832 (2013) 485–494.
[10] W. Gao, M.A. Pereira, Interleukin-6 is required for parasite specific response and host resistance to *Trypanosoma cruzi*, Int. J. Parasitol. 32 (2002) 167–170.
[11] A.R. Arocena, L.I. Onofrio, A.V. Pellegrini, A.E. Carrera Silva, A. Paroli, R.C. Cano, M.P. Aoki, S. Gea, Myeloid-derived suppressor cells are key players in the resolution of inflammation during a model of acute infection, Eur. J. Immunol. 44 (2014) 184–194.
[12] A. Mantovani, S.K. Biswas, M.R. Galdiero, A. Sica, M. Locati, Macrophage plasticity and polarization in tissue repair and remodelling, J. Pathol. 229 (2013) 176–185.
[13] D. Dal-Secco, J. Wang, Z. Zeng, E. Kolaczkowska, C.H. Wong, B. Petri, R.M. Ransohoff, I.F. Charo, C.N. Jenne, P. Kubes, A dynamic spectrum of monocytes arising from the in situ reprogramming of $CCR2^+$ monocytes at a site of sterile injury, J. Exp. Med. 212 (2015) 447–456.
[14] J.G. Tidball, S.A. Villalta, Regulatory interactions between muscle and the immune system during muscle regeneration, Am. J. Physiol. Regul. Integr. Comp. Physiol. 298 (2010) R1173–R1187.
[15] S.K. Biswas, A. Mantovani, Macrophage plasticity and interaction with lymphocyte subsets: cancer as a paradigm, Nat. Immunol. 11 (2010) 889–896.
[16] C.D. Mills, K. Ley, M1 and M2 macrophages: the chicken and the egg of immunity, J. Innate Immun. 6 (2014) 716–726.
[17] L. Antonioli, P. Pacher, E.S. Vizi, G. Hasko, CD39 and CD73 in immunity and inflammation, Trends Mol. Med. 19 (2013) 355–367.
[18] M. Lamkanfi, V.M. Dixit, Mechanisms and functions of inflammasomes, Cell 157 (2014) 1013–1022.
[19] N.J. Garg, Inflammasomes in cardiovascular diseases, Am. J. Cardiovasc. Dis. 1 (2011) 244–254.
[20] Q. Zhou, J. Yan, P. Putheti, Y. Wu, X. Sun, V. Toxavidis, J. Tigges, N. Kassam, K. Enjyoji, S.C. Robson, T.B. Strom, W. Gao, Isolated CD39 expression on $CD4^+$ T cells denotes both regulatory and memory populations, Am. J. Transplant. 9 (2009) 2303–2311.
[21] N.E. Ponce, L.M. Sanmarco, N. Eberhardt, M.C. Garcia, H.W. Rivarola, R.C. Cano, M.P. Aoki, CD73 inhibition shifts cardiac macrophage polarization toward a microbicidal phenotype and ameliorates the outcome of experimental Chagas cardiomyopathy, J. Immunol. (2016).
[22] WHO, Chagas Disease (American Trypanosomiasis), Factsheet, No 340, 2010.
[23] G.A. Schmunis, Epidemiology of Chagas disease in non-endemic countries: the role of international migration, Mem. Inst. Oswaldo Cruz 102 (Suppl. 1) (2007) 75–85.
[24] F. Nagajyothi, F.S. Machado, B.A. Burleigh, L.A. Jelicks, P.E. Scherer, S. Mukherjee, M.P. Lisanti, L.M. Weiss, N.J. Garg, H.B. Tanowitz, Mechanisms of *Trypanosoma cruzi* persistence in Chagas disease, Cell. Microbiol. 14 (2012) 634–643.
[25] R.C. Melo, C.R. Machado, *Trypanosoma cruzi*: peripheral blood monocytes and heart macrophages in the resistance to acute experimental infection in rats, Exp. Parasitol. 97 (2001) 15–23.
[26] D.L. Fabrino, L.L. Leon, G.G. Parreira, M. Genestra, P.E. Almeida, R.C. Melo, Peripheral blood monocytes show morphological pattern of activation and decreased nitric oxide production during acute Chagas' disease in rats, Nitric Oxide 11 (2004) 166–174.
[27] F. Penas, G.A. Mirkin, M. Vera, A. Cevey, C.D. Gonzalez, M.I. Gomez, M.E. Sales, N.B. Goren, Treatment in vitro with PPARalpha and PPARgamma ligands drives M1-to-M2 polarization of macrophages from *T. cruzi*-infected mice, Biochim. Biophys. Acta 1852 (2015) 893–904.
[28] C. Stempin, L. Giordanengo, S. Gea, F. Cerban, Alternative activation and increase of *Trypanosoma cruzi* survival in murine macrophages stimulated by cruzipain, a parasite antigen, J. Leukoc. Biol. 72 (2002) 727–734.
[29] C. Stempin, T. Tanos, O. Coso, F. Cerban, Arginase induction promotes *Trypanosoma cruzi* intracellular replication in Cruzipain-treated J774 cells through the activation of multiple signaling pathways, Eur. J. Immunol. 34 (2004) 200–209.
[30] H. Cuervo, M.A. Pineda, M.P. Aoki, S. Gea, M. Fresno, N. Girones, Inducible nitric oxide synthase and arginase expression in heart tissue during acute *Trypanosoma cruzi* infection in mice: arginase I is expressed in infiltrating $CD68^+$ macrophages, J. Infect. Dis. 197 (2008) 1772–1782.
[31] H. Sakaki, M. Tsukimoto, H. Harada, Y. Moriyama, S. Kojima, Autocrine regulation of macrophage activation via exocytosis of ATP and activation of P2Y11 receptor, PLoS One 8 (2013), e59778.
[32] G. Hasko, P. Pacher, Regulation of macrophage function by adenosine, Arterioscler. Thromb. Vasc. Biol. 32 (2012) 865–869.
[33] A.R. Pinto, A. Chandran, N.A. Rosenthal, J.W. Godwin, Isolation and analysis of single cells from the mouse heart, J. Immunol. Methods 393 (2013) 74–80.
[34] J. Weischenfeldt, B. Porse, Bone marrow-derived macrophages (BMM): isolation and applications, CSH Protoc. 2008 (2008) (pdb prot5080).
[35] M. Piron, R. Fisa, N. Casamitjana, P. Lopez-Chejade, L. Puig, M. Verges, J. Gascon, J. Gomez i Prat, M. Portus, S. Sauleda, Development of a real-time PCR assay for *Trypanosoma cruzi* detection in blood samples, Acta Trop. 103 (2007) 195–200.
[36] V.S. Mary, M.G. Theumer, S.L. Arias, H.R. Rubinstein, Reactive oxygen species sources and biomolecular oxidative damage induced by aflatoxin B1 and fumonisin B1 in rat spleen mononuclear cells, Toxicology 302 (2012) 299–307.
[37] L.C. Davies, S.J. Jenkins, J.E. Allen, P.R. Taylor, Tissue-resident macrophages, Nat. Immunol. 14 (2013) 986–995.
[38] Y. Shintani, A. Kapoor, M. Kaneko, R. Smolenski, F. D'Acquisto, S. Coppen, N. Harada-Shoji, H. Lee, C. Thiemermann, S. Takashima, K. Yashiro, K. Suzuki, TLR9 mediates cellular protection by modulating energy metabolism in cardiomyocytes and neurons, Proc. Natl. Acad. Sci. U. S. A. 110 (2013) 5109–5114.
[39] A. Abderrazak, T. Syrovets, D. Couchie, K. El Hadri, B. Friguet, T. Simmet, M. Rouis, NLRP3 inflammasome: from a danger signal sensor to a regulatory node of oxidative stress and inflammatory diseases, Redox Biol. 4 (2015) 296–307.
[40] M. Niederberger, P. Gines, P. Tsai, P.Y. Martin, K. Morris, A. Weigert, I. McMurtry, R.W. Schrier, Increased aortic cyclic guanosine monophosphate concentration in experimental cirrhosis in rats: evidence for a role of nitric oxide in the pathogenesis of arterial vasodilation in cirrhosis, Hepatology 21 (1995) 1625–1631.
[41] N. Ouchi, J.L. Parker, J.J. Lugus, K. Walsh, Adipokines in inflammation and metabolic disease, Nat. Rev. Immunol. 11 (2011) 85–97.
[42] P. Ataie-Kachoie, M.H. Pourgholami, D.L. Morris, Inhibition of the IL-6 signaling pathway: a strategy to combat chronic inflammatory diseases and cancer, Cytokine Growth Factor Rev. 24 (2013) 163–173.
[43] J.K. Kiecolt-Glaser, K.J. Preacher, R.C. MacCallum, C. Atkinson, W.B. Malarkey, R. Glaser, Chronic stress and age-related increases in the proinflammatory cytokine IL-6, Proc. Natl. Acad. Sci. U. S. A. 100 (2003) 9090–9095.
[44] C.K. Wong, C.Y. Ho, F.W. Ko, C.H. Chan, A.S. Ho, D.S. Hui, C.W. Lam, Proinflammatory cytokines (IL-17, IL-6, IL-18 and IL-12) and Th cytokines (IFN-gamma, IL-4, IL-10 and IL-13) in patients with allergic asthma, Clin. Exp. Immunol. 125 (2001) 177–183.
[45] J. Mauer, B. Chaurasia, J. Goldau, M.C. Vogt, J. Ruud, K.D. Nguyen, S. Theurich, A.C. Hausen, J. Schmitz, H.S. Bronneke, E. Estevez, T.L. Allen, A. Mesaros, L. Partridge, M.A. Febbraio, A. Chawla, F.T. Wunderlich, J.C. Bruning, Signaling by IL-6 promotes alternative activation of macrophages to limit endotoxemia and obesity-associated resistance to insulin, Nat. Immunol. 15 (2014) 423–430.
[46] B.E. Barton, J.V. Jackson, Protective role of interleukin 6 in the lipopolysaccharide-galactosamine septic shock model, Infect. Immun. 61 (1993) 1496–1499.
[47] D. Aderka, J.M. Le, J. Vilcek, IL-6 inhibits lipopolysaccharide-induced tumor necrosis factor production in cultured human monocytes, U937 cells, and in mice, J. Immunol. 143 (1989) 3517–3523.
[48] M. Luig, M.A. Kluger, B. Goerke, M. Meyer, A. Nosko, I. Yan, J. Scheller, H.W. Mittrucker, S. Rose-John, R.A. Stahl, U. Panzer, O.M. Steinmetz, Inflammation-induced IL-6 functions as a natural brake on macrophages and limits GN, J. Am. Soc. Nephrol. 26 (2015) 1597–1607.
[49] G. Casella, L. Garzetti, A.T. Gatta, A. Finardi, C. Maiorino, F. Ruffini, G. Martino, L. Muzio, R. Furlan, IL4 induces IL6-producing M2 macrophages associated to inhibition of neuroinflammation in vitro and in vivo, J. Neuroinflammation 13 (2016) 139.
[50] M.S. Caetano, H. Zhang, A.M. Cumpian, L. Gong, N. Unver, E.J. Ostrin, S. Daliri, S.H. Chang, C.E. Ochoa, S. Hanash, C. Behrens, IL6 blockade reprograms the lung tumor microenvironment to limit the development and progression of K-ras-mutant lung cancer, Cancer Res. 76 (2016) 3189–3199.
[51] F. Bonner, N. Borg, S. Burghoff, J. Schrader, Resident cardiac immune cells and expression of the ectonucleotidase enzymes CD39 and CD73 after ischemic injury, PLoS One 7 (2012), e34730.

[52] F. Bonner, N. Borg, C. Jacoby, S. Temme, Z. Ding, U. Flogel, J. Schrader, Ecto-5′-nucleotidase on immune cells protects from adverse cardiac remodeling, Circ. Res. 113 (2013) 301–312.
[53] J. Xaus, M. Mirabet, J. Lloberas, C. Soler, C. Lluis, R. Franco, A. Celada, IFN-gamma up-regulates the A2B adenosine receptor expression in macrophages: a mechanism of macrophage deactivation, J. Immunol. 162 (1999) 3607–3614.
[54] M.R. Elliott, F.B. Chekeni, P.C. Trampont, E.R. Lazarowski, A. Kadl, S.F. Walk, D. Park, R.I. Woodson, M. Ostankovich, P. Sharma, J.J. Lysiak, T.K. Harden, N. Leitinger, K.S. Ravichandran, Nucleotides released by apoptotic cells act as a find-me signal to promote phagocytic clearance, Nature 461 (2009) 282–286.
[55] D. Perregaux, C.A. Gabel, Interleukin-1 beta maturation and release in response to ATP and nigericin. Evidence that potassium depletion mediated by these agents is a necessary and common feature of their activity, J. Biol. Chem. 269 (1994) 15195–15203.
[56] N.V. Serbina, T. Jia, T.M. Hohl, E.G. Pamer, Monocyte-mediated defense against microbial pathogens, Annu. Rev. Immunol. 26 (2008) 421–452.
[57] W.L. Trepicchio, M. Bozza, G. Pedneault, A.J. Dorner, Recombinant human IL-11 attenuates the inflammatory response through down-regulation of proinflammatory cytokine release and nitric oxide production, J. Immunol. 157 (1996) 3627–3634.
[58] F.H. Pinto, R.D. Ribeiro, F.M. Belda Neto, J.C. do Prado Júnior, Comparative study of the behavior of infection in mice, through subcutaneous and intraperitoneal inoculation, using 2 strains of *Trypanosoma cruzi*, Rev. Saude Publica (1986).
[59] C. Bogdan, Nitric oxide and the immune response, Nat. Immunol. 2 (2001) 907–916.
[60] A.W. Taylor-Robinson, R.S. Phillips, A. Severn, S. Moncada, F.Y. Liew, The role of TH1 and TH2 cells in a rodent malaria infection, Science 260 (1993) 1931–1934.
[61] X.Q. Wei, I.G. Charles, A. Smith, J. Ure, G.J. Feng, F.P. Huang, D. Xu, W. Muller, S. Moncada, F.Y. Liew, Altered immune responses in mice lacking inducible nitric oxide synthase, Nature 375 (1995) 408–411.
[62] A. MacLean, X.Q. Wei, F.P. Huang, U.A. Al-Alem, W.L. Chan, F.Y. Liew, Mice lacking inducible nitric-oxide synthase are more susceptible to herpes simplex virus infection despite enhanced Th1 cell responses, J. Gen. Virol. 79 (Pt 4) (1998) 825–830.
[63] L.M. Sanmarco, L.M. Visconti, N. Eberhardt, M.C. Ramello, N.E. Ponce, N.B. Spitale, L. Vozza, G.A. Bernardi, S. Gea, A.R. Minguez, M.P. Aoki, IL-6 improves the nitric oxide induced-cytotoxic CD8+ T cell dysfunction in human Chagas disease, Front. Immunol. 7 (2016) 626, http://dx.doi.org/10.3389/fimmu.2016.00626.
[64] T. Tanaka, T. Kishimoto, The biology and medical implications of interleukin-6, Cancer Immunol. Res. 2 (2014) 288–294.
[65] C.A. Hunter, S.A. Jones, IL-6 as a keystone cytokine in health and disease, Nat. Immunol. 16 (2015) 448–457.